Old Dominion University
ODU Digital Commons

OEAS Faculty Publications

Ocean, Earth & Atmospheric Sciences

2010

Role of Macroscopic Particles in Deep-Sea Oxygen Consumption

Alexander B. Bochdansky
Old Dominion University, abochdan@odu.edu

Hendrik M. Van Aken

Gerhard J. Herndl

Follow this and additional works at: https://digitalcommons.odu.edu/oeas_fac_pubs

Part of the Marine Biology Commons, and the Oceanography Commons

Role of macroscopic particles in deep-sea oxygen consumption

Alexander B. Bochdansky[a,1], Hendrik M. van Aken[b], and Gerhard J. Herndl[b,c]

[a]Ocean, Earth and Atmospheric Sciences, Old Dominion University, Norfolk, VA 23529; [b]Royal Netherlands Institute for Sea Research, NL-1790 AB, Den Burg (Texel), The Netherlands; and [c]Department of Marine Biology, University of Vienna, A-1090 Vienna, Austria

Macroscopic particles (>500 μm), including marine snow, large migrating zooplankton, and their fast-sinking fecal pellets, represent primary vehicles of organic carbon flux from the surface to the deep sea. In contrast, freely suspended microscopic particles such as bacteria and protists do not sink, and they contribute the largest portion of metabolism in the upper ocean. In bathy- and abyssopelagic layers of the ocean (2,000–6,000 m), however, microscopic particles may not dominate oxygen consumption. In a section across the tropical Atlantic, we show that macroscopic particle peaks occurred frequently in the deep sea, whereas microscopic particles were barely detectable. In 10 of 17 deep-sea profiles (>2,000 m depth), macroscopic particle abundances were more strongly cross-correlated with oxygen deficits than microscopic particles, suggesting that biomass bound to large particles dominates overall deep-sea metabolism.

ecology | video analysis | marine snow | Atlantic ocean

Particles have to be of a size visible to the unaided eye before they appreciably contribute to the vertical flux in the ocean (1–3). These particles—dubbed marine snow because they resemble snowflakes in the backscatter of dive lights (4, 5)—are best enumerated by photographic means. However, microscopic and colloidal particles, a large portion of which are freely suspended bacteria and protists (6), are better quantified using optical backscatter (7). Using both techniques in tandem, we can contrast the relative distribution of microscopic and macroscopic particles in the ocean. Most video profiles in the past have been taken to a maximum depth of 1,500 m (8–10), and very few profiles exist to 4,000 m (11, 12). Thus, the data presented here, with a maximum deployment depth of 6,000 m, represent the most comprehensive basin-scale video analyses of deep-sea particles to date. To what extent and at which depth these imaged particles contribute to vertical flux remains unknown; however, a link to oxygen deficits may reflect their significance as hotspots of microbial metabolic activity.

Results and Discussion

The Archimedes III research expedition on the research vessel Pelagia was conducted from December 17, 2007 to January 16, 2008; it followed a cruise track from Fortaleza, Brazil, along the equator to the Sierra Leone Basin and then, headed northwest toward the Cape Verde Islands. The video profiles reported here were collected over a transect of ~4,000 km (Fig. 1). The Romanche Fracture Zone, the location of the greatest depth in the Mid-Atlantic Ridge, was sampled at a higher resolution than the western and eastern basins of the tropical Atlantic (Fig. 1). Microscopic particle abundance as assessed by optical backscatter generally decreased with depth, except for a pronounced peak in the oxygen minimum zone (250–500 m). Macroscopic particle numbers (>500 μm) as detected by video analysis usually decreased below the oxygen minimum zone to 2,000 m, but then, they frequently increased, forming peaks of high particle numbers (Figs. 1 and 2). Peaks were most pronounced inside the Romanche Fracture Zone, the Antarctic Bottom Water, and the two lower branches of the North Atlantic Deep Water (Figs. 1 and 2).

Selective losses of microscopic particles and the occurrence of macroscopic particle peaks in the deep sea were previously reported for the Gulf of Mexico by comparing transmissometer and video profiles (9); however, the maximum deployment depth did not exceed 1,000 m in that study.

No distinction was made between live zooplankton, fecal pellets, and aggregates with respect to particle counts. However, even in the upper 2,000 m, recognizable zooplankton shapes were rare on the video frames (i.e., <1/1,000 particles). The only discernible groups of plankton occurring in sufficient numbers to impact oxygen profiles were salps in the top 200 m of the water column. No deep layers of appendicularians or other macrozooplankton as described for the eastern Pacific (13) were apparent from our video recordings. A depth of 2,000 m, the bottom of the permanent pycnocline and below the influence of the Antarctic Intermediate Water, was selected to divide the water column into the upper and lower water masses. Depths of more than 2,000 m were well below even the deepest reaching oxygen minimum zones and are generally considered outside the influence of most actively swimming zooplankton (14). On very rare occasions, deep sea medusae, copepods, and some worm-shaped plankton were observed; however, they occurred at vanishingly small numbers below 2,000 m. Most of the particles were either too small to discern a specific shape or were amorphous marine snow particles. Only in 4 of 17 profiles were particle peaks associated with the lower part of the permanent pycnocline as described by MacIntyre et al. (15). However, we were not able to resolve small-scale features such as thin layers <5 m (16) by our method because of the roll of the ship at high seas and the transfer of its motion to the instruments. Although small-scale features are likely to occur in the deep sea, our analysis was restricted to large-scale distributions of particles.

Cross-correlations (17) between oxygen concentrations and macroscopic particles from the video recordings on one hand and oxygen concentrations and optical backscatter values on the other hand revealed that, in most cases, both particle sizes significantly and negatively cross-correlated with oxygen values at 0-m lags (Fig. 3). The observed negative relationship between particle abundance and oxygen concentration represents the well-documented oxygen consumption caused by microbial decay of organic matter characteristic of all ocean basins. In the upper 2,000 m, oxygen concentrations were significantly and more strongly negatively cross-correlated with microscopic than with macroscopic particles (paired-sample Wilcoxon signed rank test; $n = 17$; $z = -3.1$; $P = 0.002$), implying that microscopic particles dominate the oxygen drawdown in the upper 2,000 m of the water column (Fig. 3). Macroscopic particles also
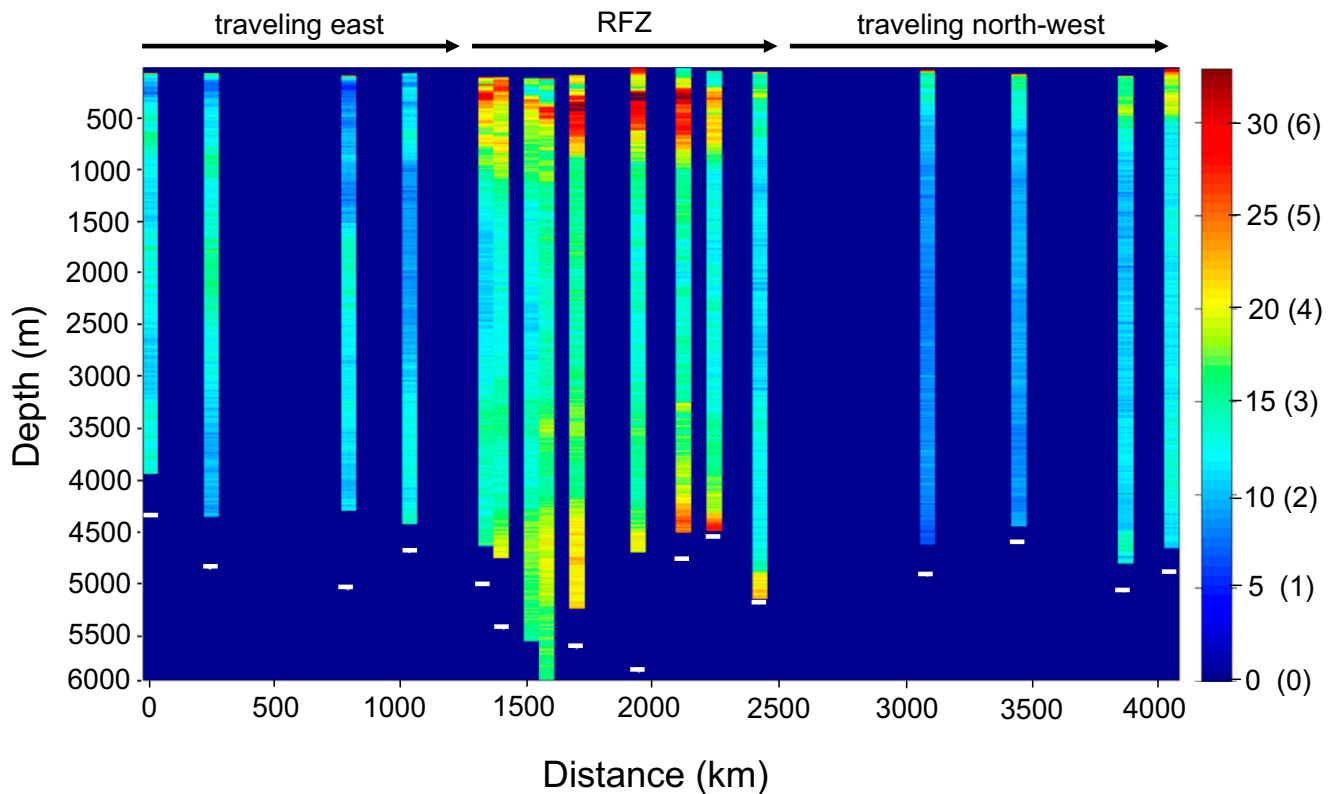
ENVIRONMENTAL SCIENCES

Fig. 1. As determined by video profiles, the relative number of particles (>500 μm) per frame, and the estimated particle number per liter (in brackets), in 100-m bins in a section across the equatorial Atlantic. White bars show the bottom depths (where bars are absent, depth exceeded 6,000 m). The euphotic zone was excluded from analysis (gaps in the top of the individual profiles), because daylight interfered with the contrast of the video images. RFZ indicates the extent of the Romanche Fracture Zone in the mid-Atlantic Ridge.

showed negative cross-correlations with oxygen concentrations but only in conjunction with microscopic particles (Fig. 4*A*). When macroscopic and microscopic particle peaks were decoupled (e.g., when their peaks were offset by several hundred meters), the oxygen deficits corresponded to the microscopic rather than the macroscopic particle peaks (Fig. 4*A*).

Below 2,000 m, however, oxygen deficits were more often associated with macroscopic than microscopic particle abundances in 10 of 17 profiles (asterisks in Fig. 3). Overall, there was no significant difference in the strengths of the correlations between the two particle sizes and oxygen below 2,000 m (paired-sample Wilcoxon signed rank test; $n = 17$; $z = -1.6$; $P = 0.113$). In this deeper layer, microbes located on macroscopic particles seem to have as much or more impact on apparent oxygen use as microscopic particles (Fig. 4*B*). In the upper 2,000 m, macroscopic particle peaks were either below the microscopic particle peaks (reflected by cross-correlation lags of an average of −75 m in the western basin; $n = 4$), above the microscopic particle peaks in the Romanche Fracture Zone (average lags of +62; $n = 9$), or relatively close to each other in the eastern basin (average lags of +23; $n = 4$), although variability was very high. The deep sea >2,000 m did not show a consistent pattern of distribution of associated particle peaks, confirming that they were mostly decoupled.

There are several possible sources for the observed macroscopic particles below 2,000 m. Within the Romanche Fracture Zone, they may have been resuspended from the canyon walls or the top of the ridge. However, macroscopic particle peaks were mostly dissociated from microscopic particle peaks, and simple resuspension of bottom material would have included small particles. Resuspension is also an insufficient explanation for peaks of macroscopic particles at stations west and east of the
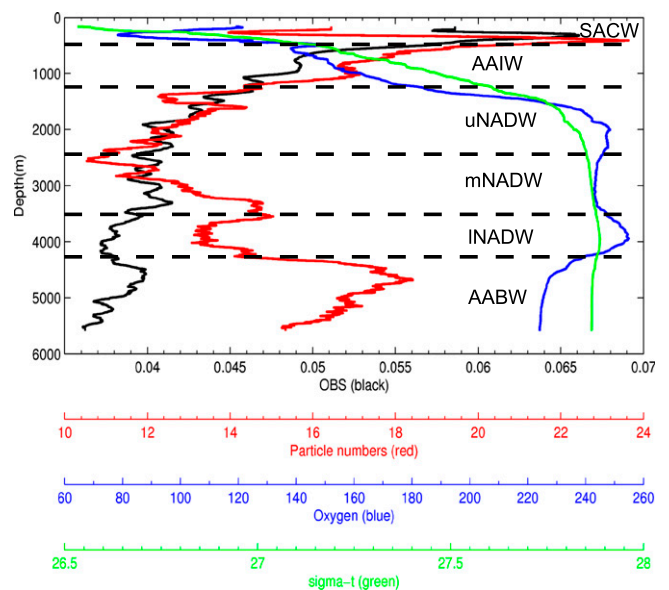

Fig. 2. Example of a deep-sea profile of sigma-t, oxygen (μmol/kg), relative particle numbers per frame from video observations (video; 100-m moving average), and optical backscatter (obs; 100-m moving average). Optical backscatter decreases with depth and remains low. In contrast, defined particle peaks in the macroscopic particle profile were present in the deep sea. Watermasses: SACW, South Atlantic Central Water; AAIW, Antarctic Intermediate Water; uNADW, upper North Atlantic Deep Water; mNADW, middle North Atlantic Deep Water; lNADW, lower North Atlantic Deep Water; AABW, Antarctic Bottom Water. The upper mixed layer is not shown.
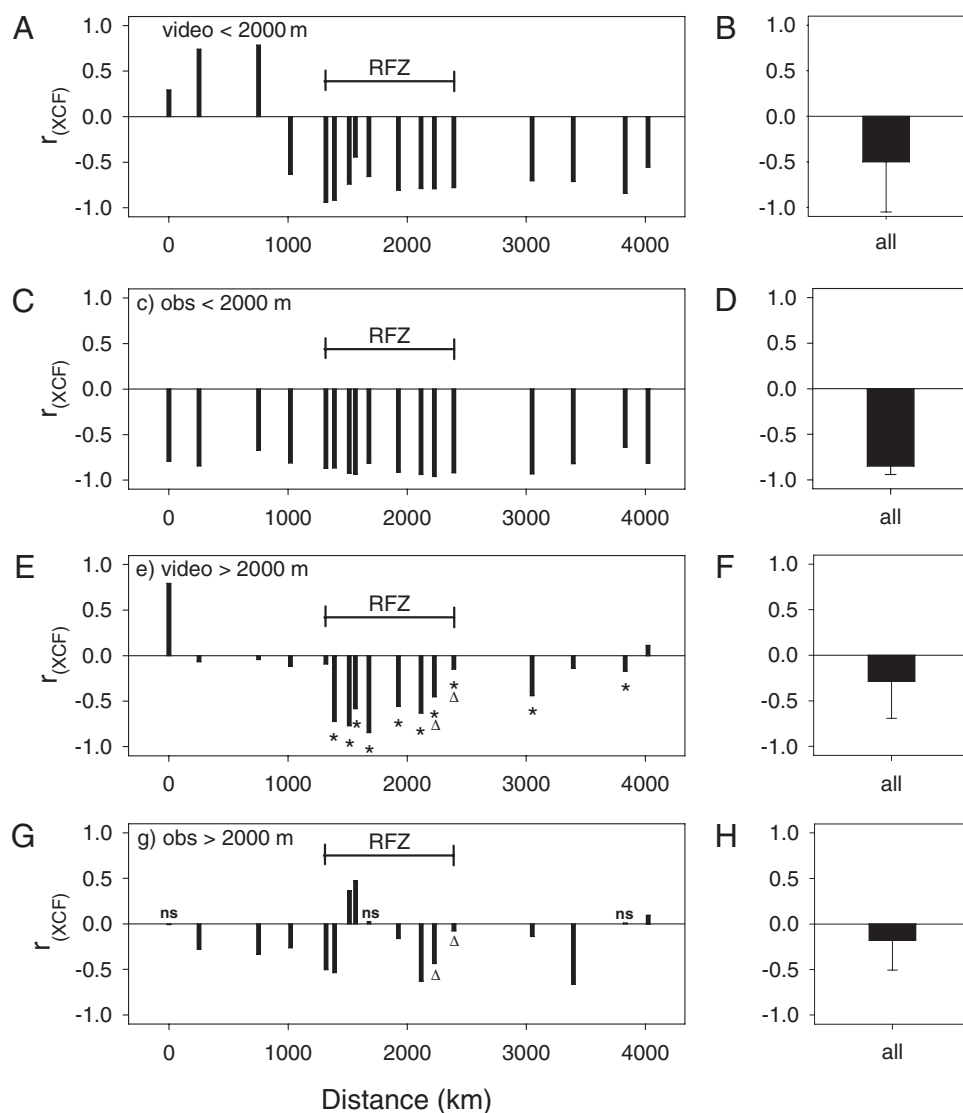
Fig. 3. Cross-correlation coefficients (r_{XCF}) of oxygen concentration versus macroscopic particles (>500 μm; video), and oxygen concentration and optical backscatter (obs). (*A–D*) Upper 2,000 m of the water column. (*E–G*) Deep sea >2,000 m. (*B, D, F,* and *H*) Means of cross-correlations of all stations with standard deviations (bars). Asterisks are negative cross-correlations between oxygen and macroscopic particles that exceeded those between oxygen and optical backscatter. All cross-correlation coefficients were significant at α = 0.05 as determined by randomizations, except those marked with ns. Triangles indicate two instances in which the presence of a deep nepheloid layer may have influenced the outcome of the cross-correlation analysis.

Romanche Fracture Zone, where particle peaks were observed in water masses thousands of meters removed from the sea floor, such as in the various branches of North Atlantic Deep Water and Antarctic Intermediate Water (Fig. 2). Horizontal transport from far away continental shelves is possible (9, 18) but requires considerable sinking to have particles entrained in layers at which we observed most of the deep-sea particle peaks. An alternative to lateral advection is that these macroscopic particles represent decayed remnants of particles originally derived from the euphotic zone and may have lost their ability to sink. Generally, however, the opposite trend (i.e., increased sinking velocity with particle age) has been observed in the ocean (19). Macroscopic particles also may reflect increased biological production, possibly at the interfaces where mixing of distinct water masses enhances biological activity (20). Among nonbiological processes, gel formation and aggregation are possible sources of macroscopic particles, and this should be considered, because the deep-sea environment provides a favorable physical and chemical environment for increased coagulation rates (21). In-

direct evidence for in situ production also comes from budget calculations showing that the amount of particulate organic carbon in the deep sea cannot be derived from sediment-trap fluxes alone (22–24).

Regardless of their origin, it is evident from our video recordings that macroscopic deep-sea particles exist in large numbers. Because episodic inputs do not affect oxygen consumption values as much as long-term processes (25), particles with an actively respiring community need to remain stationary for a significant amount of time to leave an imprint on oxygen values in the water column. Although a general relationship exists between particle size and sinking rates, there are also numerous examples where Stoke's Law does not strictly apply and even where centimeter- to meter-size particles are neutrally buoyant (26, 27). If a large portion of deep-sea particles were neutrally buoyant or slowly sinking (12), they would not appear in sediment traps or impact thorium disequilibrium profiles (28). Since oxygen consumption measured in the deep sea exceeds theoretical consumption based on concentrations of dissolved organic matter (18) and sediment-trap
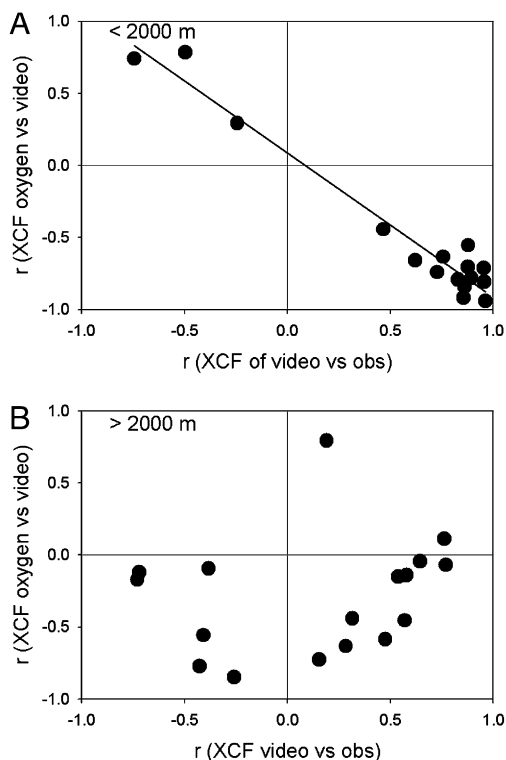
ENVIRONMENTAL SCIENCES

Fig. 4. Cross-correlation coefficients (r_{XCF}) for oxygen against macroscopic particle numbers (*y* axis) and cross-correlations between microscopic and macroscopic particles (*x* axis). (*A*) In the upper 2,000 m, microscopic and macroscopic particle peaks were strongly colocated in the water column (large positive r_{XCF}; *x* axis) with three exceptions where they were out of phase (upper left quadrant). (*B*) Below 2,000 m, microscopic and macroscopic particle peaks were more frequently decoupled, resulting in some negative values on the *x* axis (lower left quadrant). In these six cases, oxygen values were strongly and negatively cross-correlated with macroscopic particle peaks and not with microscopic particles.

flux (24, 29, 30), a disproportional role of abundant nonsinking particles—as suggested by our data—represents an additional and formidable problem for budget calculations. In addition, the size range of particles between ~50 and 500 μm may represent a significant amount of particulate matter and biomass; however, it was not accounted for with either of our methods.

In the upper water column, situations in which macroscopic particles such as marine snow dominate overall water column metabolism are rare (26). In most cases, freely suspended microbes dominate water-column respiration, and water volume-based sampling methods are justifiable. To better understand ecological processes in the deep sea, however, sampling protocols need to better account for the heterogeneity engendered by the presence of macroscopic particles. Microbial communities on particles differ taxonomically from those freely suspended in the water column (31), and physiological processes governed by diffusion and prey thresholds are influenced by substrate proximity and prey density, respectively. The possibility suggested here, that most microbial metabolism is associated with macroscopic particles, is supported by several recent observations in the deep sea. First, freely dissolved enzymatic activity is proportionally higher in the deep sea than the surface ocean, a strategy of adaptive advantage only seen where substrates are in close proximity to the microbes, such as in detrital particles (32). Second, viral abundances do not decrease with depth as rapidly as expected from the decrease of prokaryotic biomass with depth (33). Because of decreased host encounters in dilute environments, the most likely explanation for high viral

abundances is the enrichment of hosts on particles (33). Finally, a rich diversity of active deep-sea eukaryotic microbes has been reported (34). Given that most of these eukaryotes feed on prokaryotes and freely suspended prokaryotic concentrations in the deep sea drop below the threshold considered sustainable for protist feeding (35), these protists may primarily feed on prokaryotes attached to particles instead.

We conclude that the relatively strong cross-correlation between the number of macroscopic particles and oxygen concentrations in the deep sea helps to better understand some of the paradoxical observations made in this environment to date. The occurrence of large numbers of macroscopic particles in the deep sea does not represent a contradiction to estimates of particulate-carbon fluxes as long as these particles are neutrally buoyant or sink at very slow rates. These particles may represent hotspots of biological activity that, given the relative paucity of freely suspended microbial biomass, may dominate deep-sea metabolism. To better understand ecological processes of the deep sea, we need to devise new methods that take into account heterogeneity of microbial communities attached to macroscopic particles.

Materials and Methods

A black and white charge-coupled device video camera (Sentec) was mounted on a rosette frame that also held Niskin sample bottles, conductivity, temperature and oxygen probes, and an optical backscatter sensor (Seapoint turbidity meter). The camera and digital video recorder were housed in a stainless steel cylinder with a 2.54-cm-thick sapphire window (Meller Optics, Inc.) as the optical port. Two high intensity white-light emitting diodes were mounted in separate housings. Their light beams were positioned so that they intersected the field of view from both sides at ~45 ° angles. This resulted in a total light field of *ca.* 7 L visible by the camera as determined by measuring the geometry of the field of view and light cones in a dark 1,000-L experimental tank. Objects of known size (i.e., glass beads of 5-mm diameter and 10-cm plastic rectangles) were recorded on video at various distances to determine the total image volume. However, because of the tapering light intensity at the edges, the volume is only an approximation. The camera gain was set so that gelatinous zooplankton and the gelatinous matrix of marine snow particles were detectable, but more opaque particles such as hard-bodied copepods were slightly overexposed. At a shutter speed of 1/1,000 s, the camera recorded sharp images of particles at descent speeds of 1–1.5 m·s⁻¹. A customized image-analysis program based on the video editor Avidemux (Ubuntu-Linux operating system) was set to record particles larger than 6 contiguous pixels, which set the lowest detectable particle sizes at ~500 μm for particles closest to the lens. This is a frequently employed lower size threshold in video analysis of macroscopic marine particles (9, 12, 36). In essence, the video profiles represent optical backscatter tuned for particles larger than 500 μm. The lower size threshold was confirmed in the experimental tank with *Artemia nauplii* (600–700 μm in length). Depending on their reflectivity, however, smaller particles were not counted within the entire illuminated volume and thus, were underestimated. To determine the degree of undersampling of the small particles and to obtain a correction factor, we used an extrapolation of the particle-size spectrum to the smallest particle sizes by double-log transformation of particle size in pixels and number in each size bin. The smallest particles deviated predictably from the regression line. Based on this deviation, we were able to determine a correction factor of 1.43 multiplied by the observed particle number per frame over the entire particle-size spectrum. The modeled particle numbers per liter (*Nm*) were (Eq. **1**)

$$Nm[\text{numbers liter}^{-1}] = (Nv \times 1.43)/7 \qquad [\mathbf{1}]$$

where *Nv* is the number of particles per video frame, 1.43 is the correction factor over all particle sizes, and 7 L is the imaged volume per frame. The resulting estimated particle abundances per liter were similar to other deep-sea measurements using the same 500-μm lower-size threshold (9, 12). As typical for all optical measures of particle abundance (including the optical backscatter method), other factors also influence the particle counts such as geometry and reflectivity of the particles and the detection threshold used in video analysis.

For all statistical analyses, raw data in particles per video frame were used. A moving average with an unweighted 100-m window served as a low-pass filter for both optical backscatter and video data. Crosscorrelations (17), using depth instead of time (37), were performed between oxygen and particle numbers from video recordings, and between oxygen and optical backscatter values.

The cross-correlation coefficients were calculated using the *crosscorr* function (XCF) in Matlab using the equations (Eq. **2**)

$$c_{xy}(k) = \begin{cases} \dfrac{1}{n} \sum_{z=1}^{n-k} (x_z - \bar{x})(y_{z+k} - \bar{y}), & \text{where } k = 0, 1, 2, \ldots \\ \dfrac{1}{n} \sum_{z=1}^{n+k} (y_z - \bar{y})(x_{z-k} - \bar{x}), & \text{where } k = 0, -1, -2, \ldots \end{cases}$$

[2]

and (Eq. **3**)

$$r_{xy}(k) = \frac{c_{xy}(k)}{s_x s_y}, \text{ where } k = 0, \pm 1, \pm 2, \ldots$$

[3]

where *x* and *y* are the variables of the depth series to be compared (i.e., pair-wise comparison of either optical backscatter, particles per frame from the video, or oxygen concentration), *z* is depth, x-bar and y-bar are the means of the *x* and *y* series, respectively, s_x and s_y are the standard deviations of *x* and *y*, respectively, *k*

is the depth lag, *n* is the sample size, c_{xy} is the cross-covariance coefficient, and r_{xy} is the cross-correlation coefficient (labeled r_{XCF} in the figures) (17). All cross-covariance coefficients were reported for a 0 depth-lag in the figures and tested for significance at $\alpha = 0.05$ through randomizations of original data (10,000 times for each depth range and station) to create customized random frequency distributions of r_{XCF} to which the actual cross-correlation coefficients were compared and *P* values were calculated (38). Water masses were divided into surface mixed layer, Antarctic Intermediate Water, three branches of North Atlantic Deep Water (upper, middle, and lower), and Antarctic Bottom Water based on vertical distribution of potential temperature, salinity, dissolved oxygen, and dissolved nutrients (i.e., silicate, phosphate, and nitrate) (39).

1. Turner J (2002) Zooplankton fecal pellets, marine snow and sinking phytoplankton blooms. *Aquat Microb Ecol* 27:57–102.
2. Fowler SW, Knauer GA (1986) Role of large particles in the transport of elements and organic compounds through the oceanic water column. *Prog Oceanogr* 16:147–194.
3. Michaels AF, Silver MW (1988) Primary production, sinking fluxes and the microbial food web. *Deep Sea Res* 35:473–490.
4. Suzuki N, Kato K (1953) Studies on suspended materials. Marine snow in the sea I. Sources of marine snow. *Bull Faculty of Fisheries, Hokkaido Univ* 4:132–137.
5. Alldredge AL, Silver MW (1988) Characteristics, dynamics and significance of marine snow. *Prog Oceanogr* 20:41–82.
6. Azam F, Hodson RE (1977) Size distribution and activity of marine microheterotrophs. *Limnol Oceanogr* 22:492–501.
7. Battisto GM, Friedrichs CT, Miller HC, Resio DT (1999) Response of OBS to mixed grain-size suspensions during SandyDuck '97. *Coastal Sediments: Proceedings of the International Symposium on Coastal Engineering and Science of Coastal Sediment Processes*, eds Kraus NC, McDougal WG (Hauppauge, Long Island, New York), pp 297–312.
8. Gorsky G, Picheral M, Stemmann L (2000) Use of the Underwater Video Profiler for the study of aggregate dynamics in the North Mediterranean. *Estuar Coast Shelf Sci* 50:121–128.
9. Gardner W, Walsh I (1990) Distribution of macroaggregates and fine-grained particles across a continental-margin and their potential role in fluxes. *Deep Sea Res* 37:401–411.
10. Guidi L, et al. (2007) Vertical distribution of aggregates (>100 μm) and mesoscale activity in the northeastern Atlantic: Effects on the deep vertical export of surface carbon. *Limnol Oceanogr* 52:7–18.
11. Honjo S, Doherty KW, Agrawal YC, Asper VL (1984) Direct optical assessment of large amorphous aggregates (marine snow) in the deep ocean. *Deep Sea Res A* 31:67–76.
12. Asper V (1987) Measuring the flux and sinking speed of marine snow aggregates. *Deep Sea Res* 34:1–17.
13. Robison BH, Sherlock RE, Reisenbichler KR (2010) The bathypelagic community of the Monterey Canyon. *Deep Sea Res II* 57, in press.
14. Honjo S, Manganini S, Krishfield R, Francois R (2008) Particulate organic carbon fluxes to the ocean interior and factors controlling the biological pump: A synthesis of global sediment trap programs since 1983. *Prog Oceanogr* 76:217–285.
15. MacIntyre S, Alldredge AL, Gotschalk CC (1995) Accumulation of marine snow at density discontinuities in the water column. *Limnol Oceanogr* 40:449–468.
16. McManus MA, et al. (2003) Characteristics, distribution and persistence of thin layers over a 48 hour period. *Mar Ecol Prog Ser* 261:1–19.
17. Box GEP (2008) *Time Series Analysis: Forecasting and Control* (Wiley, New York).
18. Aristegui J, Gasol JM, Duarte CM, Herndl GJ (2009) Microbial oceanography of the dark ocean's pelagic realm. *Limnol Oceanogr* 54:1501–1529.
19. Berelson WM (2002) Particle settling rates increase with depth in the ocean. *Deep Sea Res II* 49:237–251.
20. Carlson CA, et al. (2004) Interactions among dissolved organic carbon, microbial processes, and community structure in the mesopelagic zone of the northwestern Sargasso Sea. *Limnol Oceanogr* 49:1073–1083.
21. Verdugo P, Santschi PH (2010) Polymer dynamics of DOC networks and gel formation in seawater. *Deep Sea Res II* 57, in press.
22. Steinberg DK, et al. (2008) Bacterial vs zooplankton control of sinking particle flux in the oceans twilight zone. *Limnol Oceanogr* 53:1327–1338.
23. Baltar F, Aristegui J, Gasol JM, Sintes E, Herndl GJ (2009) Evidence of prokaryotic metabolism on suspended particulate organic matter in the dark waters of the subtropical North Atlantic. *Limnol Oceanogr* 54:182–193.
24. Burd AB, et al. (2010) Assessing the apparent imbalance between geochemical and biochemical indicators of meso- and bathypelagic biological activity: What the @$#! is wrong with present calculations of carbon budgets? *Deep Sea Res II* 57, in press.
25. Hansell DA, Ducklow HW (2003) Bacterioplankton distribution and production in the bathypelagic ocean: Directly coupled to particulate organic carbon export? *Limnol Oceanogr* 48:150–156.
26. Herndl GJ (1988) Ecology of amorphous aggregations (marine snow) in the Northern Adriatic Sea. 2. Microbial density and activity in marine snow and its implication to overall pelagic processes. *Mar Ecol Prog Ser* 48:265–275.
27. Alldredge A, Gotschalk C (1988) In situ settling behavior of marine snow. *Limnol Oceanogr* 33:339–351.
28. Buesseler KO, et al. (2007) Revisiting carbon flux through the ocean's twilight zone. *Science* 316:567–570.
29. Ducklow H (1993) Bacterioplankton distributions and production in the northwestern Indian Ocean and Gulf of Oman, September 1986. *Deep Sea Res II* 40:753–771.
30. Reinthaler T, et al. (2006) Prokaryotic respiration and production in the meso- and bathypelagic realm of the eastern and western North Atlantic basin. *Limnol Oceanogr* 51:1262–1273.
31. DeLong EF, Franks DG, Alldredge AL (1993) Phylogenetic diversity of aggregate-attached vs. free-living marine bacterial assemblages. *Limnol Oceanogr* 38:924–934.
32. Baltar F, et al. (2010) High dissolved extracellular enzymatic activity in the deep central Atlantic Ocean. *Aquat Microb Ecol* 58:287–302.
33. Parada V, Sintes E, van Aken HM, Weinbauer MG, Herndl GJ (2007) Viral abundance, decay, and diversity in the meso- and bathypelagic waters of the North Atlantic. *Appl Environ Microbiol* 73:4429–4438.
34. Fukuda H, Sohrin R, Nagata T, Koike I (2006) Size distribution and biomass of nanoflagellates in meso- and bathypelagic layers of the subarctic Pacific. *Aquat Microb Ecol* 46:203–207.
35. Wikner J, Hagstroem A (1991) Annual study of bacterioplankton community dynamics. *Limnol Oceanogr* 36:1313–1324.
36. Goldthwait SA, Alldredge AL (2006) An investigation of diel synchronicity between water column marine snow concentration and the flux of organic matter in the Santa Barbara Channel, California. *Deep Sea Res I* 53:485–505.
37. Sutor M, Cowles T, Peterson W, Pierce S (2005) Acoustic observations of finescale zooplankton distributions in the Oregon upwelling region. *Deep Sea Res A* 52:109–121.
38. Manly BFJ (1997) *Randomization, Bootstrap, and Monte Carlo Methods in Biology* (Chapman & Hall, London).
39. Tomczak M, Godfrey JS (2003) *Regional Oceanography: An Introduction* (Butterworth-Heinemann, Boston), 2nd Ed.

ENVIRONMENTAL SCIENCES